Published in final edited form as:
IEEE Trans Control Syst Technol. 2012 July 25; 21(4): . doi:10.1109/TCST.2012.2205254.

Increasing sync rate of pulse-coupled oscillators via phase response function design: theory and application to wireless networks

Yongqiang Wang [Member,IEEE],
Department of Chemical Engineering, University of California, Santa Barbara, California USA. wyqthu@gmail.com

Felipe Núñez, and
Department of Electrical and Computer Engineering, University of California, Santa Barbara, California USA. fenunez@engineering.ucsb.edu

Francis J. Doyle III [Fellow,IEEE]
Department of Chemical Engineering, University of California, Santa Barbara, California USA. frank.doyle@icb.ucsb.edu.

Abstract

This paper addresses the synchronization rate of weakly connected pulse-coupled oscillators (PCOs). We prove that besides coupling strength, the phase response function is also a determinant of synchronization rate. Inspired by the result, we propose to increase the synchronization rate of PCOs by designing the phase response function. This has important significance in PCO-based clock synchronization of wireless networks. By designing the phase response function, synchronization rate is increased even under a fixed transmission power. Given that energy consumption in synchronization is determined by the product of synchronization time and transformation power, the new strategy reduces energy consumption in clock synchronization. QualNet experiments confirm the theoretical results.

Keywords

Synchronization rate; pulse-coupled oscillators; phase response function; wireless networks

I. Introduction

In recent years, synchronization of oscillating dynamical systems is receiving increased attention. One particular class of oscillating dynamical systems, pulse-coupled oscillators (PCOs), are of considerable interest. ‘Pulse-coupled’ means that oscillators interact with each other using pulse-based communication, i.e., they can achieve synchronization via the exchange of simple identical pulses. PCO has been used to describe many biological synchronization phenomena such as the flashing of fireflies, the contraction of cardiac cells, and the firing of neurons [1]. Recently, with the progress of ultra-wide bandwidth (UWB) impulse radio technology [2], the PCO based synchronization scheme has also been applied to synchronize wireless networks [3], [4], [5], [6]. Since it is implemented at the physical layer or MAC (Media Access Control) layer, it eliminates the high-layer intervention. Moreover, message exchanging in PCO-based synchronization strategy is independent of the origin of the pulses, which avoids requiring memory to store time information of other nodes [3]. Therefore, the PCO-based synchronization scheme has received increased attention in the communication community recently.

Despite considerable work on synchronization conditions, there remains a lack of research on the synchronization rate for PCOs, especially for PCOs with a general coupling structure other than commonly studied all-to-all structure. The synchronization rate is crucial in synchronization processes. For example, in the clock synchronization of wireless networks, the synchronization rate is a determinant of the consumption in energy, which is a precious system resource [3].

This paper analyzes the synchronization rate of weakly connected PCOs in the presence of combined global cues (also called leader, or pinner in the language of pinning control [7]) and local cues (alternatively, local coupling). The network structure is considered because in the clock synchronization of wireless networks, usually different time references are synchronized through internal interplay between different nodes and external coordination from a global time base such as GPS [8]. Due to pulsatile coupling, the synchronization rate of PCOs are very difficult to study analytically [1]. Based on the assumption of 'weakly connected', we study the problem using phase response functions. A phase response function describes the phase correction of an oscillator induced by a pulse from neighboring oscillators or external stimuli [9]. Under the assumption of weak coupling, we transform the PCO model into a simpler phase model, based on which we analyze the synchronization rate of PCOs. In fact, we will prove that the synchronization rate is determined not only by the strength of global and local cues, but also by the phase response function. This means that different phase response functions bring different synchronization rates even when the coupling strength is fixed. This has great significance for synchronization strategies such as the clock synchronization of wireless networks, where the phase response function is a design parameter. By designing the phase response function, we increase the synchronization rate under a fixed coupling strength. Given that the total energy consumption in synchronization is determined by the product of synchronization time and transmission power (corresponding to coupling strength and topology) [3], [10], the new strategy reduces energy consumption in synchronization in that synchronization time is reduced under a fixed transmission power. It is worth noting that the assumption of weak coupling is well justified by biological observations: the amplitudes of postsynaptic potentials are around 0.1 mV, which is small compared with the amplitude of excitatory postsynaptic potential necessary to discharge a quiescent cell (around 20 mV) [11]. In PCO-based wireless network synchronization schemes, weak coupling is also necessary to guarantee a robust synchronization [3].

II. Problem formulation and Model transformations

Consider a network of N pulse-coupled oscillators, which will henceforth be referred to as 'nodes'. All oscillator nodes or a portion of them can receive alignment/entrainment information from an external global cue (also called leader, or pinner in the language of pinning control [7]).

We denote the dynamics of the oscillator network as

$$\begin{aligned}\dot{x}_g &= f_g(x_g)\\ \dot{x}_i &= f_i(x_i) + g_i\delta(t-t_g) + l\sum_{1\le j\le N, j\neq i} a_{i,j}\delta(t-t_j)\ , \quad i=1,2,\ldots,N\end{aligned} \tag{1}$$

where $x_g \in [0, 1]$ and $x_i \in [0, 1]$ denote the states of the global cue and oscillator nodes, respectively. f_g and f_i describe their dynamics. $g_i \geq 0$ denotes the effect of the global cue's firing on oscillators i: when x_g reaches 1 (at time instant t_g), it fires and returns to 0, and at the same time increases oscillator i by an amount g_i. $l \geq 0$ and $a_{ij} \in \{0, 1\}$ denote the effect of oscillator j's firing on oscillator i: when x_j reaches 1 (at time instant t_j), it fires and resets to 0, and at the same time pulls oscillator i up by an amount $la_{i,j}$. The increased amount is

produced by dirac function $\delta(t)$, which is zero for all t except $t = 0$ and satisfies $\int_{-\infty}^{\infty}\delta(t)\,dt=1$.

Remark 1

If g_i (or $a_{i,j}$) is 0, then oscillator i is not affected by global cue (or oscillator j).

Assumption 1

We assume $a_{i,j} = a_{j,i}$, which is common in wireless networks [12], [13].

Assumption 2

We assume weak coupling [11], i.e., g and l satisfy $g \ll 1$ and $l \ll 1$.

Assumption 2 follows from the fact that amplitudes of postsynaptic potentials measured in the soma of neurons are far below the amplitude of the mean excitatory postsynaptic potential necessary to discharge a quiescent cell [11], it is also required in PCO-based wireless network synchronization strategies to ensure the robustness of synchronization [3].

Based on Assumption 2, the system in (1) can be described by the following phase model using the classical phase reduction technique and phase averaging technique [9], [14]:

$$\begin{aligned}\dot{\theta}_g&=w_g\\ \dot{\theta}_i&=w_i+\tfrac{g_i}{T}Q_g(\theta_g-\theta_i)+\tfrac{l}{T}\sum_{1\le j\le N, j\ne i}a_{i,j}Q_l(\theta_j-\theta_i)\ ,\quad i=1,2,\ldots,N\end{aligned}\tag{2}$$

where $\theta_g \in [0, 2\pi)$ and $\theta_i \in [0, 2\pi)$ denote the phases of global cue and oscillator i, respectively. $Q_g(x)$ and $Q_l(x)$ are phase response functions and are often referred to as phase response curves in biological study. They are periodic functions with period 2π [9], [14]. T is the period of the global cue. w_g and w_i denote the natural frequencies of global cue and oscillator i, respectively.

Remark 2

The transformation from (1) to (2) is a standard practice in the study of weakly connected PCOs and it is applicable to any limit-cycle oscillation function f_i and f_g [9]. The detailed procedure has been well documented in [14], Chapter 9 of [11], and Chapter 10 of [9].

Assumption 3

In the paper, we assume that Q_p ($p = \{l, g\}$) satisfy the following conditions:

$$Q_p(0)=0, Q_p(x)/x>0, \forall x\in(-\pi,\pi), \text{and } Q_p(-x)=-Q_p(x)\tag{3}$$

Remark 3

Assumption 3 gives an advance-delay phase response function, which is common in biological oscillators [9]. Moreover, given that in wireless networks, phase response function is a design parameter, Assumption 3 will simplify analysis and design, and as shown later, such phase response functions will also lead to good synchronization properties.

Solving the first equation in (2) gives the dynamics of the global cue $\theta_g = w_g t + \xi_g$, where the constant ξ_g denotes the initial phase of the global cue. To study if local oscillators can be

synchronized to the global cue, it is convenient to study the phase deviation of local oscillators from the global cue. So we introduce the following change of variables:

$$\theta_i = \theta_g + \xi_i = w_g t + \xi_g + \xi_i \quad (4)$$

Therefore $\xi_i \in [-\pi, \pi]$ denotes the phase deviation of the ith oscillator from the global cue. Substituting (4) into (2) yields the dynamics of phase deviations ξ_i:

$$\dot{\xi}_i = \Delta_i - \frac{g_i}{T} Q_g(\xi_i) + \frac{l}{T} \sum_{1 \le j \le N, j \ne i} a_{i,j} Q_l(\xi_j - \xi_i), \quad i = 1, 2, \ldots, N \quad (5)$$

where $\Delta_i = w_i - w_g$. In (5), the oddness property of function Q_g is exploited.

Assumption 4

In this paper, we assume $w_i = w_g$ is satisfied for all $i = 1, 2, \ldots, N$, i.e., all the oscillators have the same natural frequency as the global cue.

Using Assumption 4, (5) reduces to:

$$\dot{\xi}_i = -\frac{g_i}{T} Q_g(\xi_i) + \frac{l}{T} \sum_{1 \le j \le N, j \ne i} a_{i,j} Q_l(\xi_j - \xi_i), \quad i = 1, 2, \ldots, N \quad (6)$$

Thus far, by analyzing the properties of (6), we can obtain the roles of global and local cues as well as phase response functions in the synchronization of PCO networks:

- Synchronization: If all ξ_i asymptotically converge to 0, then we have $\theta_1 = \theta_2 = \ldots = \theta_N$ when time goes to infinity, meaning that all the nodes are synchronized to the global cue.
- Exponential bound on synchronization rate: From dynamic systems theory [15], synchronization rate is determined by the rate at which ξ_i decays to 0, namely, it can be measured by the maximal value α ($\alpha > 0$) satisfying the following inequality for some constant C:

$$\|\xi(t)\| \le Ce^{-\alpha t} \|\xi(0)\|, \quad \xi = [\xi_1 \quad \xi_2 \quad \ldots \quad \xi_N \quad]^T \quad (7)$$

  where $\| \bullet \|$ is the Euclidean norm. A larger α leads to a faster synchronization rate.

Assigning arbitrary orientation to each interaction, we can get the $N \times M$ incidence matrix B (M is the number of non-zero $a_{i,j}$ ($1 \le i \le N, j < i$), i.e., the number of interaction edges) of the interaction [16]: $B_{i,j} = 1$ if edge j enters node i, $B_{i,j} = -1$ if edge j leaves node i, and $B_{i,j} = 0$ otherwise. Then using graph theory, we can write (6) in a more compact matrix form:

$$\dot{\xi} = -\frac{1}{T} G Q_g(\xi) - \frac{l}{T} B Q_l\left(B^T \xi\right) \quad (8)$$

where ξ is given in (7), $G = \text{diag}\{g_1, g_2, \ldots, g_N\}$, and diag{•} denotes a diagonal matrix with elements {•} on the diagonal.

III. Synchronization of Pulse Coupled Oscillators

A. When all ξ_i are within $\left(-\frac{\pi}{2}, \frac{\pi}{2}\right)$

Theorem 1

For the network in (8), if all ξ_i are within $[-\varepsilon, \varepsilon]$ for some $\varepsilon \in \left[0, \frac{\pi}{2}\right)$, then the network synchronizes to the global cue when at least one g_i is positive and the local coupling topology $a_{i,j}$ is connected. Here 'connected' means that there is a multi-hop path (i.e., a sequence with nonzero values $a_{i,m_1}, a_{m_1,m_2}, \ldots, a_{m_{p-1},m_p}, a_{m_p,j}$) from each node i to every other node j.

Proof

We first prove that for any $0 \leq \varepsilon < \frac{\pi}{2}$, when $\xi \in [-\varepsilon, \varepsilon] \times \ldots \times [-\varepsilon, \varepsilon] = [-\varepsilon, \varepsilon]^N$ where × is Cartesian product, they will remain in the interval, i.e, $[-\varepsilon, \varepsilon]^N$ is positively invariant for (8). To this end, we only need to check the direction of the vector field on the boundaries. If $\xi_i = \varepsilon$, we have $0 \leq \xi_i - \xi_j \leq 2\varepsilon < \pi$ for $1 \leq j \leq N$, so from (6) and the properties of phase response functions in Assumption 3, $\dot{\xi}_i < 0$ holds. Hence vector field is pointing inward in the set, and no trajectories can escape to values larger than ε. Similarly, we can prove that when $\xi_i = -\varepsilon, \dot{\xi}_i > 0$ holds. Thus vector field is pointing inward in the set, and no trajectories can escape to values smaller than $-\varepsilon$. Therefore $[-\varepsilon, \varepsilon]^N$ is positively invariant for any $0 \leq \varepsilon < \frac{\pi}{2}$.

Next we proceed to prove synchronization. Construct a Lyapunov function as $V = \frac{1}{2}\xi^T \xi$. V is non-negative and will be zero if and only if all ξ_i are zero, meaning that all oscillators are synchronized to the global cue.

Differentiating V along trajectories of (8) yields

$$\dot{V} = \xi^T \dot{\xi} = -\frac{1}{T}\xi^T G S_1 \xi - \frac{l}{T}\xi^T B S_2 B^T \xi = -\frac{1}{T}\xi^T \left(G S_1 + l B S_2 B^T\right)\xi \quad (9)$$

where S_1 and S_2 are given by

$$S_1 = \mathrm{diag}\left\{\frac{Q_g(\xi_1)}{\xi_1}, \frac{Q_g(\xi_2)}{\xi_2}, \ldots, \frac{Q_g(\xi_N)}{\xi_N}\right\}, \quad (10)$$

$$S_2 = \mathrm{diag}\left\{\frac{Q_l\left(\left(B^T\xi\right)_1\right)}{(B^T\xi)_1}, \frac{Q_l\left(\left(B^T\xi\right)_2\right)}{(B^T\xi)_2}, \ldots, \frac{Q_l\left(\left(B^T\xi\right)_M\right)}{(B^T\xi)_M}\right\} \quad (11)$$

with $(B^T \xi)_i$ $(1 \leq i \leq M)$ denoting the ith element of the $M \times 1$ dimensional vector $B^T \xi$.

According to dynamic systems theory [15], if $GS_1 + lBS_2B^T$ in (9) is positive definite, then $\dot{V}$ is always negative when $\xi \neq 0$ and V will decay to zero exponentially, meaning that ξ will converge to zero and all oscillators are synchronized to the global cue.

Note that $(B^T \xi)_i$ $(1 \leq i \leq M)$ are in the form of $\xi_m - \xi_n$ $(1 \leq m, n \leq N)$, it follows that $(B^T \xi)_i$ are restricted to $[-2\varepsilon, 2\varepsilon]$ when all ξ_j are in $[-\varepsilon, \varepsilon]$ for some $\varepsilon \in \left[0, \frac{\pi}{2}\right)$. Given that in $(-\pi, \pi)$, $Q_g(x)$ and $Q_l(x)$ satisfies $\frac{Q_g(x)}{x} > 0$, $\frac{Q_l(x)}{x} > 0$, it follows that S_1 and S_2 are positive

definite, and thus the following inequalities are satisfied for some positive constants σ_1 and σ_2:

$$S_1 \geq \sigma_1 I, \quad S_2 \geq \sigma_2 I, \quad \sigma_1 = \min_{-\varepsilon \leq x \leq \varepsilon} \frac{Q_g(x)}{x}, \quad \sigma_2 = \min_{-2\varepsilon \leq x \leq 2\varepsilon} \frac{Q_l(x)}{x}, \quad \varepsilon \in \left[0, \frac{\pi}{2}\right) \quad (12)$$

So we have $GS_1 + lBS_2B^T \geq \sigma_1 G + \sigma_2 lBB^T$, which in combination with (9) produces

$$\dot{V} \leq -\frac{1}{T}\xi^T \left(\sigma_1 G + \sigma_2 lBB^T\right)\xi \quad (13)$$

Next we prove that $\sigma_1 G + \sigma_2 lBB^T$ is positive definite, which leads to $\dot{V} < 0$ for $\xi \neq 0$.

It can be easily verified that $\sigma_1 G + \sigma_2 lBB^T$ is of the following form:

$$\sigma_1 G + \sigma_2 lBB^T = \sigma_1 \mathrm{diag}\{g_1, g_2, \ldots, g_N\} + \sigma_2 lL \quad (14)$$

with $L \in RN \times N$ constructed as follows: for $i \neq j$, its (i, j)th element is $-a_{i,j}$, for $i = j$, its (i, j)th element is $\sum_{m=1, m\neq i}^{N} a_{i,m}$. Since σ_1, σ_2, and l are positive, and g_i, $a_{i,j}$ are non-negative, it follows from the Gershgorin Circle Theorem that $\sigma_1 G + \sigma_2 lBB^T$ only has non-negative eigenvalues [17]. Next we prove its positive definiteness by excluding 0 as an eigenvalue.

Since the topology of local coupling $a_{i,j}$ is connected, $\sigma_1 G + \sigma_2 lBB^T$ is irreducible according to graph theory [17]. This in combination with the assumption of at least one non-zero g_i guarantees that $\sigma_1 G + \sigma_2 lBB^T$ is irreducibly diagonally dominant. So from Corollary 6.2.27 of [17], we know the determinant of $\sigma_1 G + \sigma_2 lBB^T$ is non-zero and hence 0 is not its eigenvalue. Therefore $\sigma_1 G + \sigma_2 lBB^T$ is positive definite, and V will converge to 0.

B. When all ξ_i are within $(-\pi, \pi)$ and the maximal/minimal ξ_i outside $\left(-\frac{\pi}{2}, \frac{\pi}{2}\right)$

Theorem 2

For the network in (8), if all ξ_i are within $[-\varepsilon, \varepsilon]$ for some $\varepsilon \in \left[\frac{\pi}{2}, \pi\right)$ and the maximal/minimal ξ_i is outside $\left(-\frac{\pi}{2}, \frac{\pi}{2}\right)$, then the oscillator network will synchronize to the global cue when all nodes are connected to the global cue, and the following relations are satisfied:

$$g_{\min} > \frac{\sigma_4 l \lambda_{\max}\left(BB^T\right)}{\sigma_3}, \quad g_i \geq \frac{l}{\gamma_1} \sum_{1 \leq j \leq N, j \neq i} a_{i,j}\gamma_2, \quad i = 1, 2, \ldots, N \quad (15)$$

where $\lambda_{\max}$ denotes the maximal eigenvalue, $g_{\min} = \min\{g_1, g_2, \ldots, g_N\}$, and

$$\sigma_3 = \min_{-\varepsilon \leq x \leq \varepsilon} \frac{Q_g(x)}{x}, \sigma_4 = \max_{-2\varepsilon \leq x \leq 2\varepsilon} \frac{-Q_l(x)}{x}, \gamma_1 = \min_{0 \leq x \leq \varepsilon} Q_g(x), \gamma_2 = \max_{0 \leq x \leq 2\varepsilon} -Q_l(x), \varepsilon \in \left[\frac{\pi}{2}, \pi\right) \quad (16)$$

Proof

Following the direction of the proof of Theorem 1, we can prove that if the second inequality in (15) holds, then for any $\frac{\pi}{2} \leq \varepsilon < \pi$, $[-\varepsilon, \varepsilon]^N$ is positively invariant for (8), i.e.,

for $\xi \in [-\varepsilon, \varepsilon]^N$, it will always remain in the interval. Next we proceed to prove synchronization.

Choose the same Lyapunov function V as the proof of Theorem 1. Then we have

$$\dot{V} = \xi^T \dot{\xi} = -\frac{1}{T}\xi^T GS_1\xi - \frac{l}{T}\xi^T BS_2B^T\xi = -\frac{1}{T}\xi^T\left(GS_1 + lBS_2B^T\right)\xi \quad (17)$$

where S_1 and S_2 are given in (10) and (11), respectively.

When the maximal/minimal ξ_i is outside $\left(-\frac{\pi}{2}, \frac{\pi}{2}\right)$, $\xi_m - \xi_n$ ($1 \le m, n \le N$) may be outside $(-\pi, \pi)$. So in (10) and (11), the domain of $Q_g(x)$ is within $(-\pi, \pi)$, on which $Q_g(x)$ satisfies $Q_g(x)/x > 0$, and the domain of $Q_l(x)$ is not restricted to $(-\pi, \pi)$, outside of which, $Q_l(x)/x$ may be positive or negative. Therefore S_1 is still positive definite, but S_2 may be positive definite, negative definite or indefinite. From the definition of σ_3 and σ_4 in (16), we have:

$$GS_1 \ge \sigma_3 g_{\min}, \quad -lBS_2B^T \le \sigma_4 l\lambda_{\max}\left(BB^T\right)$$

Notice that $Q_l(x)$ is periodic with period 2π, and $\frac{Q_l(x)}{x} > 0$ holds for all $-\pi < x < \pi$, we know for any $\frac{\pi}{2} \le \varepsilon < \pi$, if $x_0 \in [-2\varepsilon, -\pi]$, then $Q_l(x_0) = Q_l(2\pi + x_0) \ge 0$ holds since $2\pi + x_0$ resides in the interval $[2(\pi - \varepsilon), \pi]$. Thus it follows $\frac{Q_l(x_0)}{x_0} = \frac{Q_l(x_0+2\pi)}{x_0} \le 0$, which means $\sigma_4 \ge 0$.

Therefore, (15) guarantees the positive definiteness of $GS_1 + lBS_2B^T$, and hence the synchronization of the oscillators to the global cue.

Remark 4

Theorem 2 indicates that when the maximal/minimal phase difference is outside $\left(-\frac{\pi}{2}, \frac{\pi}{2}\right)$, all oscillators have to connect to the global cue to ensure synchronization to the global cue. This is consistent with existing results which have shown that for some initial conditions (even with measure zero), PCOs cannot be synchronized by local coupling [1]. In fact, most of the existing results on PCOs are based on all-to-all connection, which amounts to $g_{\min} > 0$.

Remark 5

Theorem 2 reveals that a strong local cue does not necessarily benefit synchronization when phase difference is outside $\left(-\frac{\pi}{2}, \frac{\pi}{2}\right)$. This is also consistent with [18] which shows that synchronization may not be achieved despite arbitrarily strong local coupling.

IV. Synchronization Rate of Pulse Coupled Oscillators

Based on a similar derivation, we can get a bound on the exponential synchronization rate:

Theorem 3

For the network in (8), define σ_1, σ_2 as in (12), and σ_3, σ_4 as in (16), then

- when all ξ_i are within $[-\varepsilon, \varepsilon]$ for some $\varepsilon \in \left[0, \frac{\pi}{2}\right)$ and the conditions in Theorem 1 hold, the synchronization rate is no worse than

$$\alpha_1 = \min_{\xi} \left\{ \xi^T \left(\sigma_1 G + \sigma_2 l B B^T \right) \xi / \left(\xi^T \xi \right) \right\} T = \lambda_{\min} \left(\sigma_1 G + \sigma_2 l B B^T \right) / T \quad (18)$$

- when the maximal/minimal ξ_i is outside $\left(-\frac{\pi}{2}, \frac{\pi}{2}\right)$ and the conditions in Theorem 2 hold, the synchronization rate is no worse than

$$\alpha_2 = \left(\sigma_3 g_{\min} - \sigma_4 l \lambda_{\max} \left(B B^T \right) \right) / T \quad (19)$$

Proof

First consider the case that all ξ_i are within $[-\varepsilon, \varepsilon]$ for some $\varepsilon \in \left[0, \frac{\pi}{2}\right)$. From (9), it follows

$$\dot{V} \leq -2\alpha_1 \frac{\xi^T \xi}{2} = -2\alpha_1 V \quad (20)$$

with a_1 defined in (18), which further means that

$$V(t) \leq C^2 e^{-2\alpha_1 t} V(0) \Rightarrow \|\xi(t)\| \leq C e^{-\alpha_1 t} \|\xi(0)\| \quad (21)$$

holds for some positive constant *C*. Thus the synchronization rate is no worse than a_1 in (18).

Similarly, we can prove from (17) that when the maximal/minimal ξ_i is outside $\left(-\frac{\pi}{2}, \frac{\pi}{2}\right)$

$$V(t) \leq C^2 e^{-2\alpha_2 t} V(0) \Rightarrow \|\xi(t)\| \leq C e^{-\alpha_2 t} \|\xi(0)\| \quad (22)$$

holds for some positive constant *C*. Thus the synchronization rate is no worse than a_2 in (19).

Remark 6

When Q_g and Q_l are sinusoidal functions, all ξ_i are constrained in the interval $\left(-\frac{\pi}{2}, \frac{\pi}{2}\right)$, and there is no global cue ($G = 0$), using $\bar{\theta} = \sum_{1 \leq i \leq N} \frac{\theta_i}{N}$ as reference, we can define ξ_i as $\xi_i = \theta_i - \bar{\theta}$. Since $\xi^T 1 = 0$ with $1 = [1, 1, \ldots, 1]^T$, the constraint $\xi^T 1 = 0$ is added to the optimization $\min_{\xi} \left\{ \xi^T \left(\sigma_1 G + \sigma_2 l B B^T \right) \xi / \left(\xi^T \xi \right) \right\} / T$ in (18). Given that $G = 0$ and BB^T is the Laplacian matrix of interaction graph and hence has eigenvector 1 with associated eigenvalue 0 [17], $\lambda_{\min}$ in (18) reduces to the second smallest eigenvalue, which is the same as the convergence rate in section IV of [19] obtained using contraction analysis.

From application point of view, it is important to analyze how synchronization rate is affected by phase response function and the strengths of global and local cues. According to (16) and (19), it is clear that the synchronization rate increases with an increase in $g_{\min}$ and

$\frac{Q_g(x)}{x}$. But how phase response function and the strength of global cue affect the synchronization rate when all ξ_i are within $\left(-\frac{\pi}{2}, \frac{\pi}{2}\right)$, is not clear. (In this case, $g_{\min}$ may be zero since some oscillators may not be connected to the global cue.) In fact, we can prove that in this case the synchronization rate also increases with an increase in $\frac{Q_g(x)}{x}$ and the strength of the global cue:

Theorem 4

The synchronization rate of (8) increases with an increase in the strength of the global cue. It also increases with an increase in $\frac{Q_g(x)}{x}$.

Proof

As analyzed in the paragraph above Theorem 4, we only need to prove the statement when all $\xi_i \in [-\varepsilon, \varepsilon]$ for some $\varepsilon \in \left[0, \frac{\pi}{2}\right)$, i.e., α_1 in (18) is an increasing function of g_i and $\frac{Q_g(x)}{x}$. Recall from (14) that $\sigma_1 G + \sigma_2 lBB^T$ is an irreducible matrix with non-positive off-diagonal elements, so there exists a positive μ such that $\mu I - (\sigma_1 G + \sigma_2 lBB^T)$ is an irreducible non-negative matrix. Therefore, $\lambda_{\max}(\mu I - (\sigma_1 G + \sigma_2 lBB^T))$ is the Perron-Frobenius eigenvalue of $\mu I - (\sigma_1 G + \sigma_2 lBB^T)$ and is positive [17]. Given that for any $1 \le i \le N$, $\mu - \lambda_i(\sigma_1 G + \sigma_2 lBB^T)$ is an eigenvalue of matrix $\mu I - (\sigma_1 G + \sigma_2 lBB^T)$ where λ_i denotes the ith eigenvalue, we have

$$\mu - \lambda_{\min}\left(\sigma_1 G + \sigma_2 lBB^T\right) = \lambda_{\max}\left(\mu I - \left(\sigma_1 G + \sigma_2 lBB^T\right)\right)$$

i.e.,

$$\alpha_1 = \frac{\lambda_{\min}\left(\sigma_1 G + \sigma_2 lBB^T\right)}{T} = \frac{\mu - \lambda_{\max}\left(\mu I - \left(\sigma_1 G + \sigma_2 lBB^T\right)\right)}{T}$$

Given that the largest eigenvalue (also called the Perron-Frobenius eigenvalue) of $\mu I - (\sigma_1 G + \sigma_2 lBB^T)$ is an increasing function of any of its diagonal element [17], which is a decreasing function of g_i and $\frac{Q_g(x)}{x}$, it follows that $\lambda_{\max}(\mu I - (\sigma_1 G + \sigma_2 lBB^T))$ is a decreasing function of both g_i and $\frac{Q_g(x)}{x}$, meaning that α_1 is an increasing function of g_i and $\frac{Q_g(x)}{x}$.

Remark 7

The role of the local cue is not discussed in Theorem 4. In fact, the role of the local cue depends on the value of ξ_i: when all ξ_i are within $\left(-\frac{\pi}{2}, \frac{\pi}{2}\right)$, S_2 in (11) is positive definite, so $\xi^T B S_2 B^T \xi$ in (9) is positive, meaning that the local cue will increase the synchronization rate. Whereas when the maximal/minimal ξ_i is outside of the interval $\left(-\frac{\pi}{2}, \frac{\pi}{2}\right)$, S_2 in (11) can be positive semi-definite, negative semi-definite or indefinite, $\xi^T B S_2 B^T \xi$ in (17) can be

positive, negative or zero, thus the local cue may increase, decrease or have no influence on the synchronization rate. This conclusion is confirmed by QualNet experiments in Sec. VI.

Remark 8

From Theorem 3 and Theorem 4, one can see that in addition to the strength of coupling, i.e., g_i and l, phase response function Q_g also influences the synchronization rate. This has significant ramifications for the clock synchronization of wireless networks based on PCO-based strategies [3], [6], [10], where the phase response function is a design parameter: the synchronization rate can be increased by choosing appropriate phase response functions, even with transmission power (corresponding to coupling strength and topology) fixed, therefore leading to a reduced energy consumption. This will be addressed in Sec. V.

V. Design of Phase Response Functions

As stated in Sec. IV, the phase response function is an important determinant of the synchronization rate of PCOs. This has important ramifications for PCO-based clock synchronization strategies of wireless networks, where the phase response function is a design parameter. The PCO-based synchronization strategy is attracting increased attention in the communication community due to its low complexity [3], [6], [10]. Like in the application of most synchronization strategies, a network using a PCO-based synchronization strategy makes a distinction between an acquisition stage where the network synchronizes and the communication stage where nodes transmit and receive data [12]. In PCO-based synchronization strategies, every node of the network acts as a PCO, they interact through transmitting replicas of a pulse signal, which can be a monocycle pulse in a UWB network [3] or preambles in IEEE 802.11 networks [20]. The strategy has many advantages over conventional synchronization strategies [3]: it is implemented at the physical layer or MAC layer, which eliminates the high-layer intervention; its message exchanging is independent of the origin of the signals which avoids requiring memory to store time information of other nodes. However, in all existing PCO-based synchronization strategies, the oscillator model is directly adopted from the biological study, leading to a fixed phase response function. Our finding suggests that even under a fixed coupling strength, one can increase the synchronization rate by designing the phase response function. Given that energy consumption in a synchronization process is determined by the product of transmission power (corresponding to coupling strength and topology) and time to synchronization, our design of the phase response function can reduce the energy consumption in clock synchronization.

We focus on phase response functions in the following tanh form, for reasons outlined below:

$$Q(x) = \frac{\tanh(x/\varepsilon)}{\tanh(\pi/\varepsilon)} - \frac{x}{\pi}, \quad \text{when} \quad x \in [-\pi, \pi] \tag{23}$$

where $\varepsilon > 0$ is a free parameter and will be designed to achieve a faster synchronization rate.

Fig. 1 gives the plot of $Q(x)$ in (23). Since $Q(x)$ is 2π-periodic, only its value in the interval $[0, 2\pi]$ is plotted. $Q(x)$ is an advance-delay phase response function, i.e., external pulsatile input either delays or advances an oscillator's phase, depending upon the timing of input. Advance-delay phase response functions have been widely used in the biology community: they can well characterize the dependence of neurons' response to small depolarizations, i.e., an excitatory postsynaptic potential (EPSP) received after the refractory period delays the firing of the next spike, while an EPSP received at a later time advances the firing. The most widely-used neuron model, i.e., the Hodgkin-Huxley model, also has advance-delay

phase response functions [21]. From Theorem 4, we know in addition to the strength of the global and local cues, the phase response function of the global cue also determines the synchronization rate: the larger $\frac{Q_g(x)}{x}$ is, the faster the synchronization rate. In the following, we will show that the synchronization rate can be increased by designing ε, a parameter in the phase response function.

Theorem 5

For the pulse-coupled oscillator network in (8) and the phase response function of the global cue in the form of (23), if all ξ_i are within $(-\pi, \pi)$, the synchronization rate increases with a decrease in ε, no matter whether the maximal/minimal ξ_i is within or outside $\left(-\frac{\pi}{2}, \frac{\pi}{2}\right)$.

Proof

According to Theorem 4, the synchronization rate increases with an increase in $\frac{Q_g(x)}{x}$. So we only need to prove that $\frac{Q_g(x)}{x}$ increases with a decrease in ε for $x \in (-\pi, \pi)$.

Using the tanh type phase response function, we have

$$\frac{Q_g(x)}{x} = \frac{\tanh(x/\varepsilon)}{x\tanh(\pi/\varepsilon)} - \frac{1}{\pi}, \quad x \in (-\pi, \pi) \quad (24)$$

Since $\frac{Q_g(x)}{x}$ in (24) is a smooth function of ε, we can calculate its derivative with respect to ε:

$$\frac{d\left(\frac{Q_g(x)}{x}\right)}{d\varepsilon} = \frac{\pi \operatorname{sech}^2\left(\frac{\pi}{\varepsilon}\right)\tanh\left(\frac{x}{\varepsilon}\right) - x\operatorname{sech}^2\left(\frac{x}{\varepsilon}\right)\tanh\left(\frac{\pi}{\varepsilon}\right)}{x\varepsilon^2\tanh^2\left(\frac{\pi}{\varepsilon}\right)} \quad (25)$$

To that prove $\frac{Q_g(x)}{x}$ increases with a decrease in ε, we need to prove that $\frac{d\left(\frac{Q_g(x)}{x}\right)}{d\varepsilon}$ is negative. Since $\varepsilon^2\tanh^2\left(\frac{\pi}{\varepsilon}\right)$ is positive, we only need to prove that (26) is negative for $-\pi < x < \pi$:

$$\frac{1}{x}\left(\pi\operatorname{sech}^2\left(\frac{\pi}{\varepsilon}\right)\tanh\left(\frac{x}{\varepsilon}\right) - x\operatorname{sech}^2\left(\frac{x}{\varepsilon}\right)\tanh\left(\frac{\pi}{\varepsilon}\right)\right) \quad (26)$$

Using properties of hyperbolic functions, we can rewrite (26) as follows:

$$\frac{4}{\left(e^{\frac{\pi}{\varepsilon}} + e^{\frac{-\pi}{\varepsilon}}\right)^2\left(e^{\frac{x}{\varepsilon}} + e^{\frac{-x}{\varepsilon}}\right)^2} \times \frac{\pi\left(e^{\frac{2x}{\varepsilon}} - e^{\frac{-2x}{\varepsilon}}\right) - x\left(e^{\frac{2\pi}{\varepsilon}} - e^{\frac{-2\pi}{\varepsilon}}\right)}{x} \quad (27)$$

hence the problem is reduced to proving the negativity of $f(x, \varepsilon)$ in (28) for $-\pi < x < \pi$.

$$f(x,\varepsilon) \triangleq \frac{\pi\left(e^{\frac{2x}{\varepsilon}} - e^{\frac{-2x}{\varepsilon}}\right) - x\left(e^{\frac{2\pi}{\varepsilon}} - e^{\frac{-2\pi}{\varepsilon}}\right)}{x} \quad (28)$$

Using a Taylor expansion, equation (28) can be further rewritten as

$$\begin{aligned} f(x,\varepsilon) &= \frac{1}{x}\left[2\pi\left(\frac{2x}{\varepsilon} + \frac{\left(\frac{2x}{\varepsilon}\right)^3}{3!} + \frac{\left(\frac{2x}{\varepsilon}\right)^5}{5!} + \dots\right) - 2x\left(\frac{2\pi}{\varepsilon} + \frac{\left(\frac{2\pi}{\varepsilon}\right)^3}{3!} + \frac{\left(\frac{2\pi}{\varepsilon}\right)^5}{5!} + \dots\right)\right] \\ &= \frac{2}{x}\left(\frac{\pi\left(\frac{2x}{\varepsilon}\right)^3 - x\left(\frac{2\pi}{\varepsilon}\right)^3}{3!} + \frac{\pi\left(\frac{2x}{\varepsilon}\right)^5 - x\left(\frac{2\pi}{\varepsilon}\right)^5}{5!} + \dots\right) \end{aligned} \quad (29)$$

which is negative for all x in $-\pi < x < \pi$.

So $\frac{\left(\frac{Q_g(x)}{dx}\right)}{d\varepsilon}$ is negative, thus $\frac{Q_g(x)}{x}$ increases with a decrease in ε, which completes the proof.

VI. QualNet Experiments

We use a high-fidelity network evaluation tool (QualNet) to illustrate the proposed strategy. QualNet is a commercial network platform that can be used to evaluate wireless networks. It was released by Scalable Network Technologies and has been widely used to predict the performance of MANETs, satellite networks and sensor networks, among others [22].

In the implementation, we constructed a wireless network composed of 19 nodes (including 1 global cue). Each node has a counter as clock and stores the phase response function (as shown in Fig. 1) in a lookup table. Upon receiving a pulse, a node shifts its phase by an amount determined by its current time and the phase response function in the lookup table. The structure of the network is illustrated in Fig. 2, where node number 0 is the global cue. A broadcasting-based MAC layer protocol is adopted to establish the pulse based communication between different nodes, which is represented by the circles in Fig. 2. Although a broadcasting scheme is used, the communication in the network is not all-to-all due to limited transmission range. The interaction topology is also illustrated in Fig. 2, which can be verified to be a connected graph.

We first considered the case where $\xi_i \in \left(-\frac{\pi}{2}, \frac{\pi}{2}\right)$. From Theorem 1, all nodes can synchronize to the global cue if at least one g_i is non-zero. To confirm the prediction, we only connected oscillator 1 to the global cue with $g_1 = 0.01$. We set the natural frequency to 2π, the strength of local coupling to $l = 0.01$, and implemented the PCO network under different phase response functions in (23), i.e., different pairs of ε_g (ε in Q_g) and ε_l (ε in Q_l). The network was synchronized, confirming Theorem 1. To illustrate our phase-response-function based design strategy, we recorded the average time to synchronization from 100 runs for each pair of ε_g and ε_l. In each run, we set the initial value of the global cue as 0 and chose the initial values of local nodes randomly from a uniform distribution on $\left(-\frac{\pi}{2}, \frac{\pi}{2}\right)$. The times to synchronization are given by the first element of each 2-tuple in Table I. We can see that synchronization rate increases with a decrease in ε_g, which confirms the theoretical results in Sec. V. The total energy consumption in synchronization process is also recorded and averaged over the 100 runs. The results are given by the second element of each 2-tuple in Table I. With a decrease in ε_g, the energy consumption indeed decreases, which confirms the effectiveness of our design methodology in Sec. V.

Using the same setup, we also implemented the network when the maximal/minimal ξ_i is outside $\left(-\frac{\pi}{2}, \frac{\pi}{2}\right)$. We ran the implementation for 100 times and each time chose the initial values of ξ_i randomly from a uniform distribution on $(-\pi, \pi)$. 28 of the 100 runs were unsynchronized, confirming Theorem 2 that all oscillators have to be connected to the global cue to guarantee synchronization. So we made $g_1 = g_2 = \ldots = g_N = 0.01$ and re-ran the implementation under different phase response functions. The results are given in Table II. With a decrease in ε_g, the energy consumption indeed decreases, confirming the effectiveness of our design methodology in Sec. V. Moreover, using the same coupling strength, we also implemented the network under Peskin's phase response function used in [3], and obtained a (synchronization time, energy consumption) 2-tuple as (25.24, 489.59). Since it is larger than the smallest energy consumption in Table II, which is obtained under the same coupling strength, this confirms that by tuning the parameter ε_g in phase response function, energy consumption can indeed be reduced.

Setting $g_1 = g_2 = \ldots = g_N = g$, $\varepsilon_g = 0.4$, and $\varepsilon_l = 0.05$, we also implemented the network under different strengths of global and local cues, i.e., different pairs of g and l. For each pair of g and l, we ran the implementation for 100 times, and each time we chose the initial values of ξ_i randomly from a uniform distribution on $(-\pi, \pi)$. The average time to synchronization is given by the first element of each 2-tuple in Table III. From Table III, we can see that a larger g indeed leads to a faster synchronization rate (a smaller synchronization time), whereas a larger l does not necessarily bring a faster synchronization rate. A larger l may even desynchronize the network when g is small (as illustrated by the last two elements of the first row). This confirms the analytical results in Remark 7, which state that the local cue may increase or decrease the synchronization rate. The same conclusion can be drawn for energy consumption, which is given by the second element of each 2-tuple in Table III.

VII. Conclusions

The synchronization rate of pulse-coupled oscillators is analyzed. It is proven that in addition to the strengths of global and local cues, phase response function also determines synchronization rate. This inspires us to increase the synchronization rate by choosing an appropriate phase response function, when the phase response function is a design parameter. An application is the clock synchronization of wireless networks, to which pulse-coupled synchronization strategies have been successfully applied. We give a new design methodology for pulse-coupled synchronization of wireless networks. It can reduce energy consumption in clock synchronization. QualNet experiments are given to illustrate the analytical results.

Acknowledgments

The work was supported in part by U.S. Army Research Office through Grant W911NF-07-1-0279, National Institutes of Health through Grant GM078993, and the Institute for Collaborative Biotechnologies through grant W911NF-09-0001 from the U.S. Army Research Office. The content of the information does not necessarily reflect the position or the policy of the Government, and no official endorsement should be inferred.

References

[1]. Mirollo R, Strogatz S. Synchronization of pulse-coupled biological oscillators. SIAM J. Appl. Math. 1990; 50:1645–1662.

[2]. Abdrabou A, Zhuang W. A position-based QoS routing scheme for UWB mobile ad hoc networks. IEEE J. Sel. Areas Commun. 2006; 24:850–855.

[3]. Hong YW, Scaglione A. A scalable synchronization protocol for large scale sensor networks and its applications. IEEE J. Sel. Areas Commun. 2005; 23:1085–1099.

[4]. Tyrrell A, Auer G, Bettstetter C. Emergent slot synchronization in wireless networks. IEEE. Trans. Mob. Comput. 2010; 9:719–732.

[5]. Werner-Allen, G.; Tewari, G.; Patel, A.; Welsh, M.; Nagpal, R. Proc. SenSys 05. USA: 2005. Firefly inspired sensor network synchronicity with realistic radio effects; p. 142-153.

[6]. Pagliari R, Hong YWP, Scaglione A. Bio-inspired algorithms for decentralized round-robin and proportional fair scheduling. IEEE J. Sel. Areas Commun. 2010; 28:564–575.

[7]. Delellis P, di Bernardo M, Porfiri M. Pinning control of complex networks via edge snapping. Chaos. 2011; 21:033119. [PubMed: 21974654]

[8]. Kopetz H, Ochsenreiter W. Clock synchronization in distributed real-time systems. IEEE Trans. Comput. 1987; C-36:933–940.

[9]. Izhikevich, E. Dynamical systems in neuroscience: the geometry of excitability and bursting. MIT Press; London: 2007.

[10]. Barbarossa S, Scutari G. Bio-inspired sensor network design: Distributed decision through self-synchronization. IEEE Signal Process. Mag. 2007; 24:26–35.

[11]. Hoppensteadt, FC.; Izhikevich, EM. Weakly connected neural networks. Springer; New York: 1997.

[12]. Rappaport, TS. Wireless communications: principles and practice. Prentice Hall; New York: 2002.

[13]. Park, SJ.; Sivakumar, R. GLOBECOM. Taibei: 2002. Load-sensitive transmission power control in wireless ad-hoc networks; p. 42-46.

[14]. Vreeswijk CV, Abbott LF, Ermentrout GB. When inhibition not excitation synchronizes neural firing. J. Comput. Neurosci. 1994; 1:313–321. [PubMed: 8792237]

[15]. Khalil, HK. Nonlinear systems. Prentice Hall; New Jersey: 2002.

[16]. Godsil, C.; Royle, G. Algebraic graph theory. Springer; New York: 2001.

[17]. Horn, R.; Johnson, C. Matrix analysis. Cambridge University Press; London: 1985.

[18]. Monzón, P.; Paganini, F. Global considerations on the Kuramoto model of sinusoudally coupled oscillators. Proc. 44th IEEE Conf. Decision Control; Spain. 2005. p. 3923-3928.

[19]. Chung, S.; Slotine, J. On synchronization of coupled Hopf-Kuramoto oscillators with phase delays. Proc. 49th IEEE Conf. Decision Control; USA. 2010. p. 3181-3187.

[20]. Tyrrell, A.; Auer, G.; Bettstetter, C. Fireflies as role models for synchronization in ad hoc networks. Proc. Int. Conf. Bio Inspired Models of Network, Information and Computing Systems (BIONETICS); Italy. 2006. p. 1-7.

[21]. Ermentrout B. Type I membrances, phase resetting curves, and synchrony. Neural Comput. 1996; 8:979–1001. [PubMed: 8697231]

[22]. QualNet 4.5 User's Guide. Scalable networks inc.; 2008. http://www.scalable-networks.com

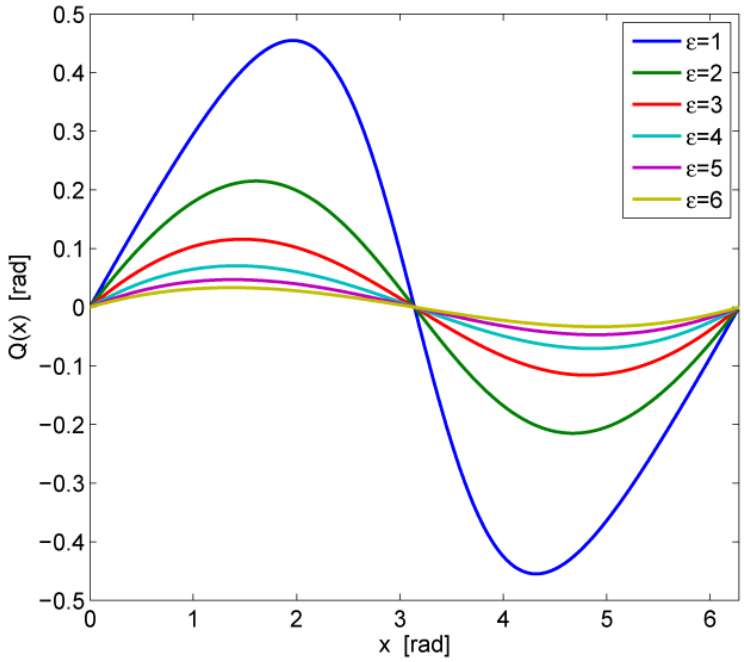

Fig. 1.
The shape of tanh type advance-delay phase response functions in equation (23).

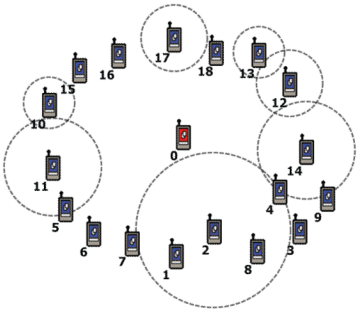

	1	2	3	4	5	6	7	8	9	10	11	12	13	14	15	16	17	18
1		1	1	1	1	1	1	1	1	0	1	0	0	0	0	0	0	0
2	1		1	1	1	1	1	1	1	0	0	0	0	1	0	0	0	0
3	1	1		1	0	0	1	1	1	0	0	1	1	1	0	0	1	1
4	1	1	1		0	0	1	1	1	0	0	1	1	1	0	0	1	1
5	1	1	0	0		1	1	0	0	1	1	0	0	0	1	1	0	0
6	1	1	0	0	1		1	0	0	1	1	0	0	0	1	1	0	0
7	1	1	1	1	1	1		1	0	1	1	0	0	0	0	0	0	0
8	1	1	1	1	0	0	1		1	0	0	1	1	1	0	0	0	1
9	1	1	1	1	0	0	0	1		0	0	1	1	1	0	0	1	1
10	0	0	0	0	1	1	1	0	0		1	0	0	0	1	1	1	0
11	1	0	0	0	1	1	1	0	0	1		0	0	0	1	1	0	0
12	0	0	1	1	0	0	0	1	1	0	0		1	1	0	0	1	1
13	0	0	1	1	0	0	0	1	1	0	0	1		1	0	1	1	1
14	0	1	1	1	0	0	0	1	1	0	0	1	1		0	0	1	1
15	0	0	0	0	1	1	1	0	0	1	1	0	0	0		1	1	1
16	0	0	0	0	1	1	1	0	0	1	1	0	1	0	1		1	1
17	0	0	1	1	0	0	0	0	1	1	0	1	1	1	1	1		1
18	0	0	1	1	0	0	0	1	1	0	0	1	1	1	1	1	1	

Fig. 2.

Schematic of the network (left) and interaction matrix (right) used in the QualNet implementation. In the interaction matrix, ‘1’ denotes interaction between two nodes, and ‘0’ denotes no interaction.

TABLE I

Time to synchronization [s](1st element of each 2-tuple) and energy consumption [10^{-3}J](2nd element of each 2-tuple) under different phase response functions $\left(\xi_i \in \left(-\frac{\pi}{2}, \frac{\pi}{2}\right), l{=}g_1{=}0.01, g_2{=}g_3{=}\ldots{=}g_N{=}0\right)$

$\varepsilon_g \setminus \varepsilon_l$	**0.05**	**0.1**	**0.2**	**0.4**	**0.8**	**1.6**
0.4	(37.23, 729.39)	(36.76, 719.99)	(36.55, 715.79)	(36.23, 709.05)	(35.83, 701.39)	(43.37, 852.19)
0.8	(37.88, 742.39)	(37.40, 732.79)	(37.88, 742.39)	(36.73, 719.39)	(36.44, 713.59)	(44.04, 865.59)
1.6	(38.17, 748.19)	(37.90, 742.79)	(38.38, 752.39)	(37.62, 737.19)	(36.83, 721.43)	(45.76, 899.99)

TABLE II

Time to synchronization [s](1st element of each 2-tuple) and energy consumption [10^{-3}J](2nd element of each 2-tuple) under different phase response functions ($\xi_i \in (-\pi, \pi)$, $l = g_1 = g_2 = \ldots = g_N = 0.01$)

$\varepsilon_g \setminus \varepsilon_l$	**0.05**	**0.1**	**0.2**	**0.4**	**0.8**	**1.6**
0.4	(22.93, 443.39)	(23.17, 448.19)	(23.14, 447.59)	(22.58, 436.39)	(21.53, 415.39)	(22.44, 433.59)
0.8	(24.95, 483.79)	(25.21, 488.99)	(25.36, 491.99)	(24.23, 469.39)	(23.63, 457.39)	(24.34, 471.59)
1.6	(30.14, 587.59)	(31.92, 623.19)	(31.75, 619.79)	(30.35, 519.79)	(28.15, 547.79)	(29.09, 566.59)

TABLE III

Time to synchronization [s] (1st element of each 2-tuple) and energy consumption [10^{-3}J] (2nd element of each 2-tuple) under different strengths of global and local cues ($\xi_i \in (-\pi, \pi)$, $g_1 = g_2 = \ldots = g_N = g$)

$g \setminus l$	**0.01**	**0.02**	**0.03**	**0.04**	**0.05**	**0.06**
0.01	(22.93, 443.39)	(23.21, 448.99)	(26.37, 512.19)	(27.26, 529.99)	(no sync, −)	(no sync, −)
0.02	(17.49, 334.59)	(18.90, 362.79)	(22.03, 425.39)	(24.60, 476.79)	(24.38, 472.39)	(21.39, 412.59)
0.03	(14.18, 268.39)	(14.99, 284.59)	(18.03, 345.39)	(19.93, 383.39)	(20.35, 391.79)	(19.91, 382.99)